Green's function retrieval with Marchenko equations: a sensitivity analysis.

Jan Thorbecke, Joost van der Neut † and Kees Wapenaar ‡, Delft University of Technology, Department of Geoscience and Engineering, Section of Applied Geophysics, The Netherlands*

SUMMARY

Recent research showed that the Marchenko equation can be used to construct the Green's function for a virtual source position in the subsurface. The method requires the reflection response at the surface and an estimate of the direct arrival of the wavefield, traveling from the virtual source location to the acquisition surface. In this paper, we investigate the sensitivity of this method. We demonstrate its robustness with respect to significant amplitude and phase errors in the direct arrival. The erroneous operators introduce low amplitude artefacts. The main reflections and internal multiples are still presents and disturbing ghost events are not introduced. In case the reflection data is modeled in a medium with losses, ghost events seem to be visible in the upgoing wavefield, but not in the downgoing wavefield.

Introduction

A new approach to retrieve the Green's function for a virtual source in the subsurface, from measured data at the surface, is introduced by Broggini et al. (2012a,b); Wapenaar et al. (2012a). The method is based on Marchenko-type equations and the virtual wavefield is constructed by an iterative scheme. The reconstructed wavefield contains all internal multiples and is equal to the complete Green's function of a virtual source in the subsurface. Using reciprocity, from here onward we treat the virtual source as a virtual receiver. The up- and downgoing wavefields at the virtual receiver position can be constructed by combining different results of the iterative scheme. These up- and downgoing fields are the input for algorithms that allow imaging without artefacts from internal multiples. The underlying theory has been derived for the 3D situation by Wapenaar et al. (2013) and more applications of the method are now rapidly being developed (Slob et al., 2013; van der Neut et al., 2013; Behura et al., 2012).

To start the iterations, the method requires, besides the measured data at the surface, an estimate of the direct arrival at the surface from the virtual position in the subsurface. The measured data at the surface has to be free of free-surface multiples and it is assumed that the medium is lossless. In this paper we investigate the robustness of the method with respect to errors in the estimate of the direct arrival, and the influence of intrinsic losses in the medium. The influence is analyzed in the retrieved up- and down-going wavefields at the virtual receiver position. The following numerical studies are carried out:

- amplitude and phase errors of the direct arrival due to a velocity error in the model,
- amplitude errors of the direct arrival,
- with a reflection response for a medium with losses.

These sensitivity studies are a first step towards applying the method on real data. Using real data we expect to have estimates of direct arrivals, which can deviate significantly from a correct operator. By having an idea what the influence is of an erroneous direct arrival, we expect to take these effects into account in further processing steps.

Theory

In the brief theoretical background given in this section, we follow Wapenaar et al. (2012a) and only present the final outcome of the scheme for 2-dimensional media. The iterative scheme starts with an estimate of the direct arrival between the surface ($\mathbf{x}_0$), and the virtual receiver position $\mathbf{x}_F = (x_F, z_F)$ in the subsurface. The time-reversal of this direct arrival is the downgoing $p_0^+(\mathbf{x}_0, \mathbf{x}_F, t)$. Convolved with the reflection response of the medium $R(\mathbf{x}_0, \mathbf{x}, t)$, this results in an upgoing field at the surface:

$$p_0^-(\mathbf{x}_0, \mathbf{x}_F, t) = \int_x \int_{t'} R(\mathbf{x}_0, \mathbf{x}, t - t') p_0^+(\mathbf{x}, \mathbf{x}_F, t') \mathrm{d}t' \mathrm{d}\mathbf{x} \quad (1)$$

where $R(\mathbf{x}_0, \mathbf{x}, t)$ is the measured reflection response without surface-related multiples and deconvolved for the source wavelet. In the iterative scheme, the downgoing field is updated with a time-reversed and windowed version of $p_{k-1}^-(\mathbf{x}_0, \mathbf{x}_F, t)$, according to:

$$p_k^+(\mathbf{x}_0, \mathbf{x}_F, t) = p_0^+(\mathbf{x}_0, \mathbf{x}_F, t) - w(\mathbf{x}_0, t) p_{k-1}^-(\mathbf{x}_0, \mathbf{x}_F, -t) \quad (2)$$

where $w(\mathbf{x}_0, t)$ is a window function as explained in Wapenaar et al. (2012a) and k the iteration number. After several iterations (in the examples shown in this paper, 10-15 iterations are sufficient), using construction equation (1) and (with subscript 0 replaced by k) update equation (2), the wavefield converges. The summation of the time-reversed final downgoing field and the final upgoing field is proportional to the Green's function at a virtual receiver at position $\mathbf{x}_F$ (Wapenaar et al., 2013).

Based on the same equations, but with a change in the sign, a slightly different scheme is carried out as well. The update equation in this scheme is

$$q_k^+(\mathbf{x}_0, \mathbf{x}_F, t) = p_0^+(\mathbf{x}_0, \mathbf{x}_F, t) + w(\mathbf{x}_0, t) q_{k-1}^-(\mathbf{x}_0, \mathbf{x}_F, -t) \quad (3)$$

where $q_k^+(\mathbf{x}_0, \mathbf{x}_F, t)$ is the so-called symmetric counterpart of equation (2). The final outcome of equations (2) and (3) are combined to create down- and upgoing Green's functions:

$$\begin{aligned} G^{+,+}(\mathbf{x}_F, \mathbf{x}_0, t) =& \tfrac{1}{2}\{p^-(\mathbf{x}_0, \mathbf{x}_F, t) + p^+(\mathbf{x}_0, \mathbf{x}_F, -t)\} \\ &+ \tfrac{1}{2}\{-q^-(\mathbf{x}_0, \mathbf{x}_F, t) + q^+(\mathbf{x}_0, \mathbf{x}_F, -t)\} \quad (4) \\ G^{-,+}(\mathbf{x}_F, \mathbf{x}_0, t) =& \tfrac{1}{2}\{p^-(\mathbf{x}_0, \mathbf{x}_F, t) + p^+(\mathbf{x}_0, \mathbf{x}_F, -t)\} \\ &- \tfrac{1}{2}\{-q^-(\mathbf{x}_0, \mathbf{x}_F, t) + q^+(\mathbf{x}_0, \mathbf{x}_F, -t)\} \quad (5) \end{aligned}$$

In the examples below, these up- and downgoing wavefields are computed for different approximations of the initial downgoing wavefield $p_0^+(\mathbf{x}_0, \mathbf{x_F}, t)$, and with a reflection response

$R(\mathbf{x}_0, \mathbf{x}, t)$ modeled in a medium with losses. The obtained up- and downgoing Green's functions can be the input for a migration scheme (Wapenaar et al., 2012b; van der Neut et al., 2013), where internal multiples are included.

Modeling experiments

A simple model, shown in Figure 1, is created to illustrate the method. In this model, the density contrast between the layers is chosen very high to generate strong internal multiples. In Figure 2, the reflection response of the medium, for a source at the surface at $\mathbf{x} = 0$, is shown.

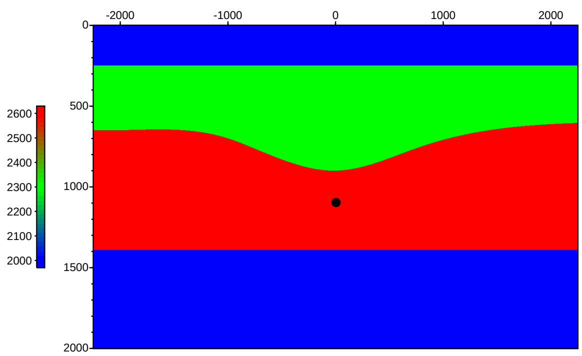

Figure 1: Velocity model for finite difference modeling of the input data set of the Marchenko iterations. Sources and receivers are placed at the surface x[-2250, 2250] with a 10 m distance. A virtual receiver is placed at x=0, z=1100 m. The density of the layers is alternating between 1000 and 5000 kg/m^3.

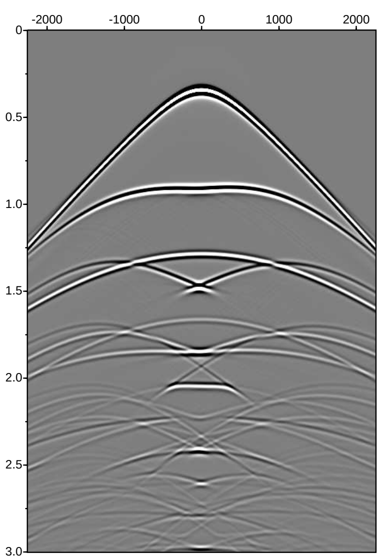

a) $R(\mathbf{x}_0, \mathbf{x}, t)$

Figure 2: The input reflection data $R(\mathbf{x}_0, \mathbf{x}, t)$ convolved with a Ricker wavelet. Free surface multiples are not included. Note the strong internal multiples.

Figure 3 shows the result obtained under ideal conditions. In this case, the direct arrival is computed, with finite difference in the correct medium, to construct the initial downgoing $p_0^+(\mathbf{x}_0, \mathbf{x}_F, t)$. The left panel shows the downgoing field, with on top the maximum amplitude at the first arrival time. The middle panel shows the computed downgoing Green's function and the right panel the upgoing Green's function, after 15 iterations.

The next experiment is carried out with a velocity error of $+15\%$ in the first layer of the model. Due to this velocity error, the operator p_0^+ does not focus to a band-limited point, but to a blurred focal area. The computed wavefields, shown in Figure 4b,c, contains the same events as in Figure 3b,c, and the only differences are some more pronounced artefacts and a time delay due to the velocity error.

The results in Figure 5 are based on the correct velocity model to calculate the direct arrival in p_0^+, but the amplitude along the first arrival time is made constant (top of Figure 5a). The effect of this amplitude error is barely visible in the downgoing $G^{+,+}$ in Figure 5b, but introduces a few errors in the upgoing $G^{-,+}$ in Figure 5c. Note that the construction equation (1) includes an integration over the (limited) receiver array at the surface. In the examples above we have not used any tapers at the edges of the acquisition domain. It is expected that tapering the edges of the acquisition domain will reduce some of the artifacts in the results (for example the indicated event in Figure 5c).

For the last experiment in this paper, the correct direct arrival time and amplitude are used for p_0^+, but the reflection response R is modeled in a medium with losses (Q=50). In the theoretical derivation of the iterative scheme, it is assumed the the medium is lossless and it is expected that in this case the method will not give correct results. However, Figure 6 shows that the downgoing Green's function does not have any visible extra ghost events and only in the upgoing field ghost events are introduced (indicated with an arrow in Figure 6c). We expect that these can be reduced by applying a Q compensation to the reflection data prior to running the iterative scheme.

Conclusion and discussion

The experiments in this paper indicate that the introduced scheme to calculate the up- an downgoing Green's functions at a virtual receiver in the subsurface, from reflection data and the direct arrival is robust. The scheme does not diverge and remains stable in case the focusing operator has errors in phase and amplitude. In case the reflection data is modeled in a medium with losses, ghost events are visible in the retrieved upgoing field only, but not in the retrieved downgoing field. These ghost events can probably be reduced by applying Q-compensation.

Acknowledgements

We are thankful to research school ISES for supporting this research.

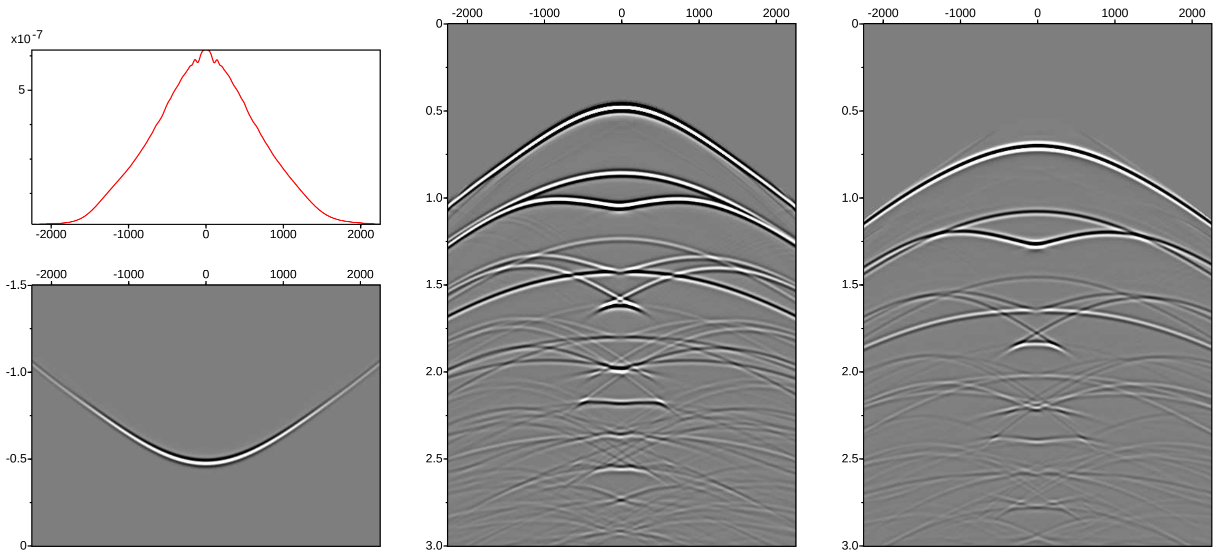

a) $p_0^+(\mathbf{x}_0,\mathbf{x}_F,t)$ b) $G^{+,+}(\mathbf{x}_F,\mathbf{x}_0,t)$ c) $G^{-,+}(\mathbf{x}_F,\mathbf{x}_0,t)$

Figure 3: Up- and downgoing wavefields after 15 iterations.This is the reference result with the correct direct propagating field (p_0^+ (a)) and R computed for a medium without losses. The edges of the lateral integration (over $\mathbf{x}$) are not tapered and introduces small truncation artifacts visible before the first arrival in the upgoing Green's function $G^{-,+}$ (c).

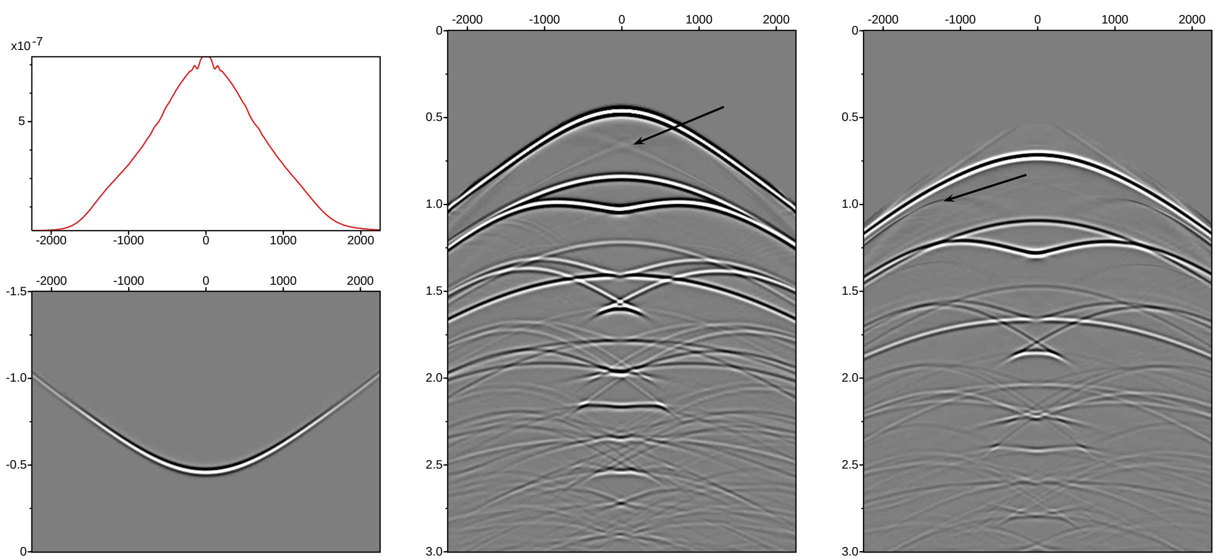

a) $p_0^+(\mathbf{x}_0,\mathbf{x}_F,t)$ b) $G^{+,+}(\mathbf{x}_F,\mathbf{x}_0,t)$ c) $G^{-,+}(\mathbf{x}_F,\mathbf{x}_0,t)$

Figure 4: Up- and downgoing wavefields after 15 iterations with an error in the velocity model to calculate p_0^+ . The velocity in the top layer of the model has been increased from 2000 to 2300 m/s. In comparison with the reference results a few artefacts are introduced, which are indicated with an arrow in the upgoing field (c).

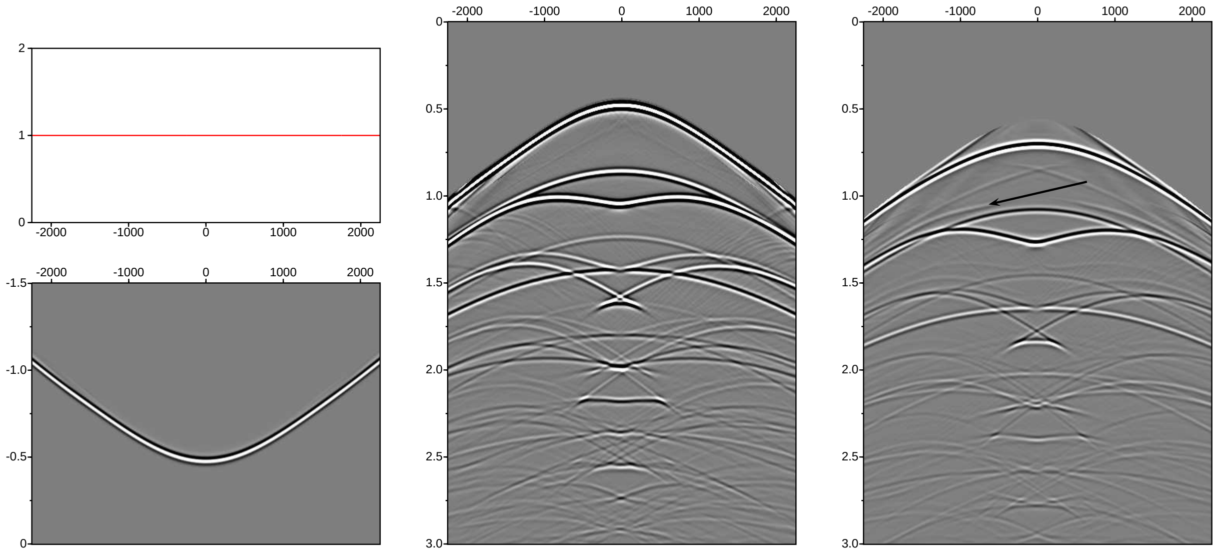

a) $p_0^+(\mathbf{x}_0, \mathbf{x}_F, t)$ b) $G^{+,+}(\mathbf{x}_F, \mathbf{x}_0, t)$ c) $G^{-,+}(\mathbf{x}_F, \mathbf{x}_0, t)$

Figure 5: Up- and downgoing wavefields after 15 iterations with an amplitude error in p_0^+. The amplitude along the wavefield is flat for all offsets as shown in the amplitude plot in (a). In the upgoing Green's function (c) only a few ghosts events, with a low amplitude and indicated with an arrow, are introduced.

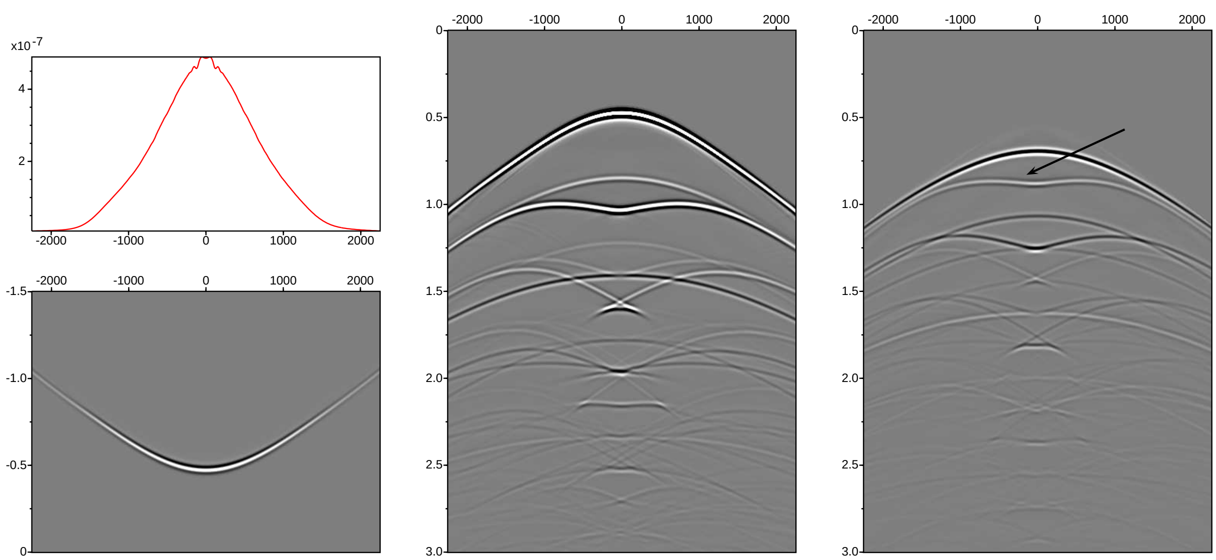

a) $p_0^+(\mathbf{x}_0, \mathbf{x}_F, t)$ b) $G^{+,+}(\mathbf{x}_F, \mathbf{x}_0, t)$ c) $G^{-,+}(\mathbf{x}_F, \mathbf{x}_0, t)$

Figure 6: Up- and downgoing wavefields after 15 iterations. The reflection data is modeled in a medium with losses (Q=50). This violation of the theoretical assumption of a lossless medium introduces extra ghosts events (indicated with an arrow), which are visible in the upgoing wavefield (c), but not in the downgoing wavefield (b).

REFERENCES

Behura, J., Wapenaar, K., and Snieder, R., 2012, Newton-Marchenko-Rose Imaging: 82nd Annual International Meeting, SEG, Expanded Abstracts, SPMI 5.7.

Broggini, F., R. Snieder and K. Wapenaar, 2012a, Creating a virtual source inside a medium from reflection data with internal multiples: a stationary-phase analysis: 82nd Annual International Meeting, SEG, Expanded Abstracts, ST 1.4.

Broggini, F., R. Snieder, and K. Wapenaar, 2012b, Focusing the wavefield inside an unknown 1d medium: Beyond seismic interferometry: Geophysics, **77**, A25-A28.

Slob, E., K. Wapenaar, F. Broggini, and R. Snieder, 2013, Seismic reflector imaging while eliminating internal multiples using Marchenko-type equations: Geophysics, 78, submitted.

van der Neut, J., E. Slob, K. Wapenaar, J. Thorbecke, R. Snieder and F. Broggini, Interferometric redatuming of autofocused primaries and internal multiples, 2013: 83th Annual International Meeting, SEG, submitted

Wapenaar, K., F. Broggini, and R. Snieder, 2012b, Creating a virtual source inside a medium from reflection data: heuristic derivation and stationary-phase analysis: Geophysical Journal International, **190**, 1020-1024.

Wapenaar, K., J. Thorbecke, J. van der Neut, E. Slob, F. Broggini, J. Behura, and R. Snieder, 2012b, Integrated migration and internal multiple elimination: 82nd Annual International Meeting, SEG, Expanded Abstracts, SPMUL 1.5.

Wapenaar, K., F. Broggini, E. Slob, and R. Snieder, 2013a, Three-dimensional single-sided Marchenko inverse scattering, data-driven focusing, Greens function retrieval and their mutual relations: Physical Review Letters, **110**, 084301.